uc3m | Universidad Carlos III de Madrid
Department of Aerospace Engineering

PhD Aerospace Engineering UC3M
Doctoral Meetings 2026

uc3m PHD

Theoretical and numerical analysis of the plasma response in a 10-kW class applied-field magnetoplasmadynamic thruster (AF-MPD)

Manuel Ferrazzani
Supervisors: Eduardo Ahedo, Davide Poli

Applied-field Magnetoplasmadynamic thrusters (AF-MPDs)

- Composed of an **annular anode** and a **multichannel tubular cathode**.
- An electrical current is imposed between the two electrodes in order to ionize the propellant which is injected from the backplate and/or from the cathode.
- An **external magnetic field**, supplied by either a coil or a permanent magnet, is used to accelerate the plasma:
  - Both the discharge current $\boldsymbol{j}$ and the applied magnetic field $\boldsymbol{B_a}$ are axial and radial $\boldsymbol{j} = j_z\mathbf{1_z} + j_r\mathbf{1_r}$, $\boldsymbol{B_a} = B_z\mathbf{1_z} + B_r\mathbf{1_r}$.
  - If the magnetic field is strong enough, the plasma undergoes a rotation motion in the θ-direction (Hall current):

$$\boldsymbol{j_\theta} = \beta_e \frac{\boldsymbol{j} \times \boldsymbol{B_a}}{B_a}$$

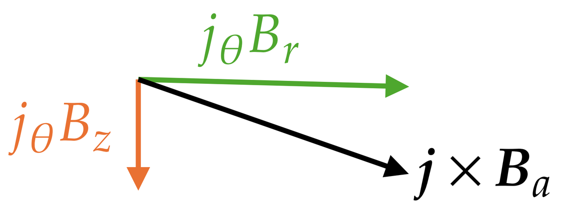

  where $\beta_e(B_a)$ is called **Hall parameter**.
  - The induced Hall current and the applied magnetic field produce both a **pinching** ($\boldsymbol{F} = j_\theta B_z \mathbf{1_r}$) and a **blowing** ($\boldsymbol{F} = j_\theta B_r \mathbf{1_z}$) motion.
  - If the discharge current is very high (> 500 A), then the plasma itself generates a magnetic field in the θ-direction strong enough to accelerate the plasma thanks to Lorentz force $\boldsymbol{F} = \boldsymbol{j} \times \boldsymbol{B_{ind}}$.
- In recent years, several **low-power AF-MPD** (< 10 kW) designs employing **hollow cathodes** instead of tubular cathodes have been built and tested.
- As the self-field component is negligible, these thrusters are more similar to Cylindrical Hall Thrusters (CHTs) or Electrodeless Plasma Thrusters (EPTs).
- Experimental evidences shows that **performances of low-power AF-MPDs are poor**.

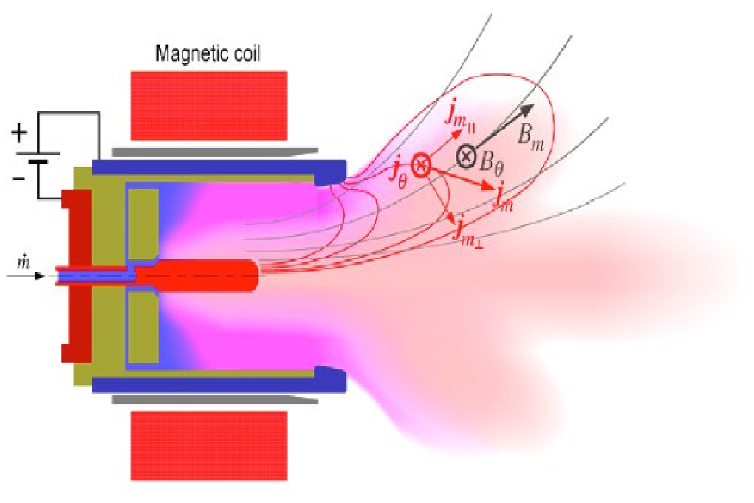

Andrenucci (2010). *Encyclopedia of Aerospace Engineering*

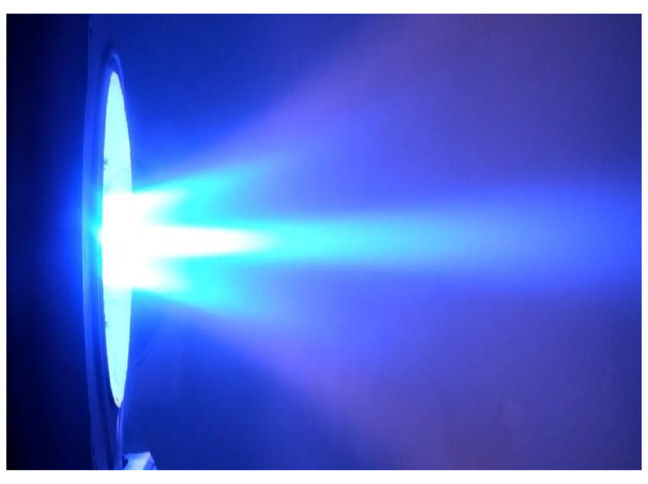

Boxberger et al. (2017). *Integral Measurements of 100 kW Class Steady State Applied-Field Magnetoplasmadynamic Thruster SX3 and Perspectives of AF-MPD Technology*

Research gap and Objectives

- Several authors have proposed **models to estimate the thrust** of AF-MPDs. However, the underlying physical mechanisms responsible for plasma acceleration are still not fully understood.
- **Scaling laws** for AF-MPD thrusters **are inaccurate** in predicting the performances in terms of the geometry and of the operative parameters, especially for in the low-power regime.
- **Technical literature on numerical simulations** of AF-MPD thrusters is practically inexistent.

The thesis aims at:

- **Characterizing the acceleration mechanisms** of low-power AF-MPD thrusters, which are still unclear.
- Analyzing the plasma response to **identify sources of efficiency losses** to improve future designs.
- **Comparing the performances** with other classes of plasma thrusters such as Hall thrusters, Cylindrical Hall thrusters and Electrodeless Plasma Thrusters, and high power AF-MPDs.

Methodology and preliminary results

- Numerical simulations have been performed with **HYPHEN**, an in-house made 2D axisymmetric hybrid code.
- HYPHEN adopts a **Particle in Cell** (**PIC**) model for heavy species (ions, neutrals) for which a **cartesian mesh** is used and a fluid model for electrons which employs a so-called **Magnetic Field Aligned Mesh** (**MFAM**) to reduce numerical diffusion.
- A **xenon-fed low-power AF-MPD** design proposed by **Sasoh et al.** has been simulated.

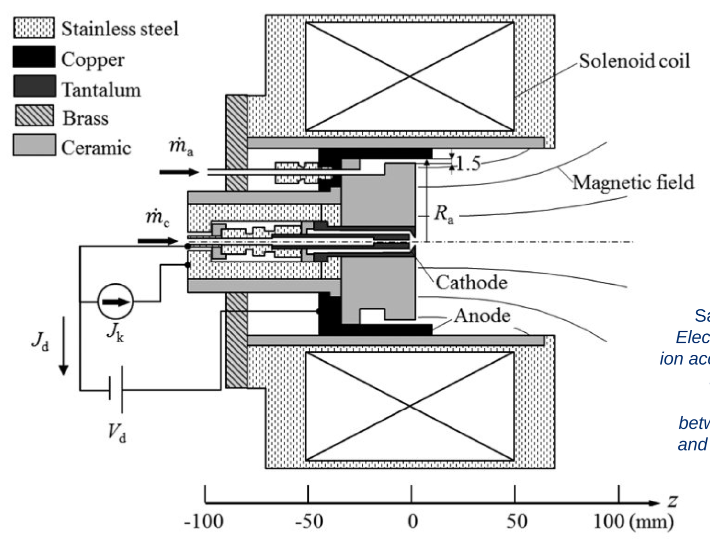

Sasoh et al. (2017). *Electrostatic/magnetic ion acceleration through a slowly diverging magnetic nozzle between a ring anode and an on-axis hollow cathode*

$\dot{m}_a$	$\dot{m}_c$	V_d	B_a	J_d	F	I_{sp}	P_d	η_t
2.73 mg/s	0.49 mg/s	150 V	0.2 T	6.2 A	26.9 mN	835 s	930 W	0.121

Simulation results

Plasma response

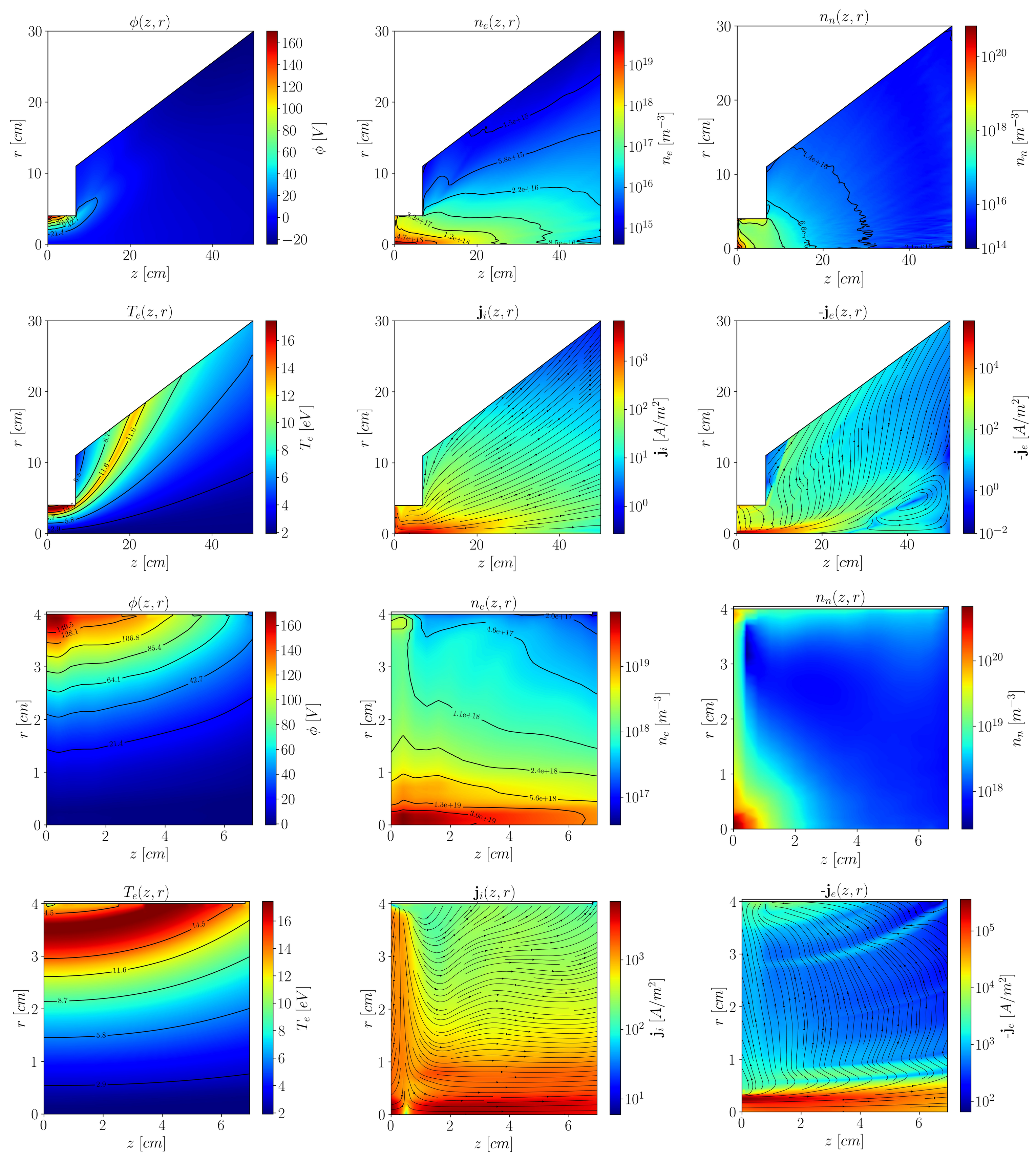

Propulsive performances

F	I_d	P_d
27.32 mN	6.44 A	994.12 W

η_t	η_{ene}	η_{div}	η_{disp}	η_u	η_{cur}	η_{prod}
0.117	0.307	0.508	0.746	0.961	0.398	0.343

Simulation setup

PIC mesh

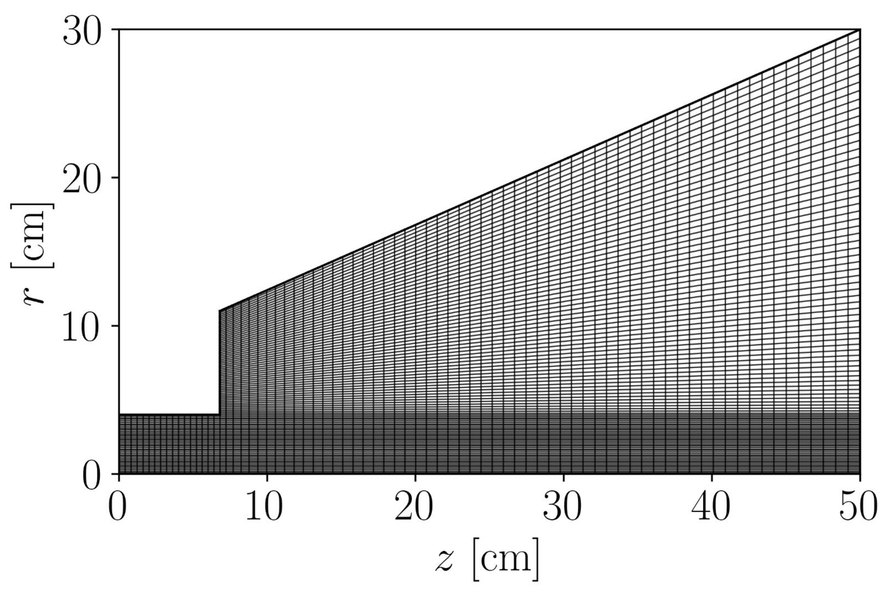

MFAM

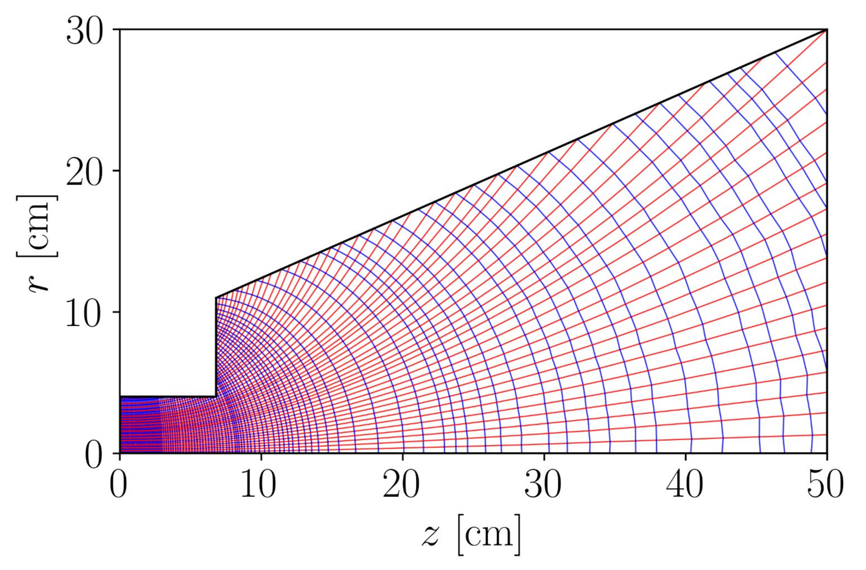

Simulation parameters

Domain size (z, r)	$(50, 30)$ cm
PIC mesh number of cells	6521
MFAM number of cells	2929
Ion-moving time step	15 ns
Simulation steps	90000
Injected Xe velocity	300 m/s
Injection Xe temperature	850 K
Walls accommodation factor	1

Reaction set

$Xe + e^- \longrightarrow Xe^+ + 2e^-$
$Xe + e^- \longrightarrow Xe^{2+} + 3e^-$
$Xe + e^- \longrightarrow Xe^{3+} + 4e^-$
$Xe^+ + e^- \longrightarrow Xe^{2+} + 2e^-$
$Xe^+ + e^- \longrightarrow Xe^{3+} + 3e^-$

$Xe^{2+} + e^- \longrightarrow Xe^{3+} + 2e^-$
$Xe(s) + Xe^+(f) \longrightarrow Xe^+(s) + Xe(f)$
$Xe(f) + e^- \longrightarrow Xe^+ + 2e^-$
$Xe^+(s) + e^- \longrightarrow Xe^{2+} + 2e^-$
$Xe^+(s) + e^- \longrightarrow Xe^{3+} + 3e^-$

PhD Student: - Manuel Ferrazzani – mferrazz@ing.uc3m.es
Supervisor: Eduardo Ahedo – eahedo@ing.uc3m.es
Supervisor: Davide Poli – dpoli@pa.uc3m.es